Jurnal Teknologi

Full Paper

INVESTIGATION OF MECHANICAL AERATOR PARAMETERS ON THE POND WATER FLOW RATE USING CFD

Mohd Azlan Musa[a,b,c], Fatin Alias[a], Muhammad Faris Roslan[a], Nora Azlina[a], Ahmad Fitriadhy[a], Anuar Abu Bakar[a], Mohammad Fadhli Ahmad[a], Mohd Asamudin A. Rahman[a,b], Che Wan Mohd Noor[a]*

[a]Faculty of Ocean Engineering Technology, Universiti Malaysia Terengganu, 21030 Kuala Nerus, Terengganu, Malaysia
[b]Centre for Offshore Renewable Energy (CEFORE)Universiti Malaysia Terengganu, 21030 Kuala Nerus, Terengganu, Malaysia
[c]Institute of Oceanography and Environment (INOS)Universiti Malaysia Terengganu, 21030 Kuala Nerus, Terengganu, Malaysia

Article history
Received
19 March 2025
Received in revised form
6 July 2025
Accepted
9 July 2025
Published Online
16 June 2026

*Corresponding author
che.wan@umt.edu.my

Graphical abstract

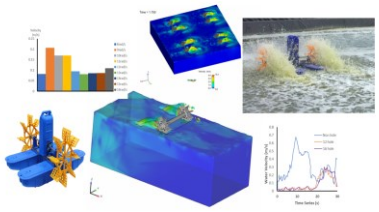

Abstract

Mechanical aerators are essentialfor enhancing water circulation and dissolved oxygen (DO) levels in shrimp pond aquaculture, which are critical for shrimp health and growth. Among the common aerator types, including paddlewheel, diffuser, and propeller systems, paddlewheels are widely used due to their effectiveness in surface aeration. However, uncontrolled flow rates may lead to pond erosion and excessive energy consumption. This study investigates the influence of paddlewheel design parameters on pond water flow rates using Computational Fluid Dynamics (CFD) simulations in FLOW-3D. Three paddle configurations (with 12 holes, 16 holes, and no holes), rotational speeds ranging from 8 to 16 rad/s, and two layout setups (inline and parallel) were analyzed. The results show a strong correlation between paddle speed and flow rate, with optimal performance observed between 9 and 11 rad/s. The design without holes produced up to 73.3% higher flow rates but led to unbalanced circulation. In contrast, the parallel configuration provided more uniform flow distribution than the inline setup, helping to maintain consistent DO levels and reduce localized stagnation. These findings offer practical insights into optimizing aerator design and operation to improve water quality, minimize erosion risk, and support sustainable shrimp aquaculture.

Keywords: Mechanical aerator, CFD, Pond Flow rate, Paddle Configuration, Hydrodynamic Performance

Abstrak

Aerator mekanikal adalah penting untuk meningkatkan peredaran air dan paras oksigen terlarut (DO) dalam akuakultur kolam udang, yang amat kritikal untuk kesihatan dan pertumbuhan udang. Antara jenis aerator yang biasa digunakan termasuklah sistem paddlewheel, penyebar, dan kipas, di mana paddlewheel paling meluas digunakan kerana keberkesanannya dalam pengudaraan permukaan. Walau bagaimanapun, kadar aliran yang tidak terkawal boleh menyebabkan hakisan kolam dan penggunaan tenaga yang berlebihan. Kajian ini menyiasat pengaruh parameter reka bentuk paddlewheel terhadap kadar aliran air kolam menggunakan simulasi Dinamik Bendalir Pengiraan (CFD) dalam perisian FLOW-3D. Tiga konfigurasi pendayung (dengan 12 lubang, 16 lubang, dan tanpa lubang), julat kelajuan putaran antara 8 hingga 16 rad/s, dan dua susun atur (sejajar dan selari) telah dianalisis. Hasil kajian menunjukkan hubungan yang

kuat antara kelajuan paddle dan kadar aliran, dengan prestasi optimum dicapai pada julat 9 hingga 11 rad/s. Reka bentuk tanpa lubang menghasilkan peningkatan kadar aliran sehingga 73.3%, namun menyebabkan peredaran air yang tidak seimbang. Sebaliknya, konfigurasi selari memberikan taburan aliran yang lebih sekata berbanding konfigurasi sejajar, membantu mengekalkan paras DO yang konsisten dan mengurangkan kawasan bertakung. Penemuan ini memberikan panduan praktikal dalam mengoptimumkan reka bentuk dan operasi aerator bagi meningkatkan kualiti air, mengurangkan risiko hakisan, dan menyokong kelestarian akuakultur udang.

Kata kunci: Aerator mekanikal, CFD, Kadar aliran kolam, Konfigurasi pendayung, Prestasi hidrodinamik

1.0 INTRODUCTION

The mechanical aerator is a pivotal rotary device extensively employed within shrimp ponds to treat the water quality. Among the various types, paddlewheels emerge as a significant variant of mechanical aerators as shown in Figure 1. These paddlewheel aerators operate by partially submerging in water, affixed onto a floater and are integrated with a rotating motor positioned along a horizontal axis [1]. Activation of these aerators, typically through electrical power, initiates continuous rotation, facilitating the mixing of air with the water via surface contact thereby improving dissolved oxygen (DO) levels essential for the vitality of aquatic organisms.

Traditionally, paddlewheel aerators are designed with specific features, such as rotors, floaters, and perforated blades, to facilitate effective water aeration [2]. Each component is carefully engineered to ensure optimal functionality, such as perforations (hole)number are strategically placed along paddle surface to enables the efficient induction of air into the water [3].

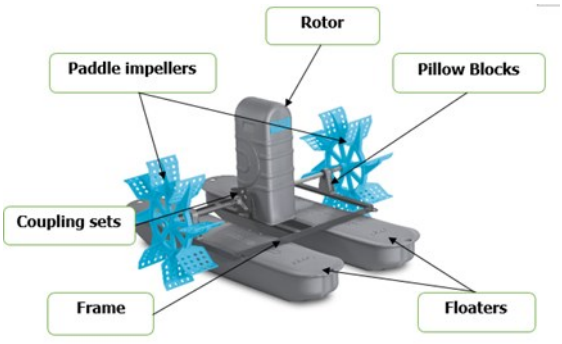

Figure 1 1 Hp Paddlewheel Aerator

Despite their effectiveness on functionality, there is still significant challenges remain in optimizing the DO levels in the waters [4]. Whereas, the effectiveness of aeration systems in maintaining DO levels is commonly evaluated by using two key performance metrics: Standard Oxygen Transfer Rate (SOTR), which quantifies the amount of oxygen transferred into water per hour, and Standard Aeration Efficiency (SAE), which represents the oxygen transferred per unit of energy consumed (kg O_2/kWh). These metrics, defined by Equations (1) and (2), are critical indicators of an aerator's operational performance in aquaculture systems:

$$SOTR = K_{La} \cdot V \cdot (C^* - C) \quad \text{(Eqn. 1)}$$

$$SAE = SOTR / P \quad \text{(Eqn. 2)}$$

Where K_{La} is the oxygen transfer coefficient (h^{-1}), V is the volume of water, C^* and C are the saturated and actual DO concentrations, respectively, and P is the power input. Among of these variables, K_{La} is most sensitive to hydrodynamic conditions, particularly turbulence, which is influenced by the rotor speed and flow rate generated by the aerator. As rotor speed increases, so does turbulence and surface renewal, enhancing oxygen transfer.

In shrimp pond systems, the water flow rate induced by paddlewheel aerators plays a pivotal role in governing SOTR and SAE. Adequate flow enhances oxygen diffusion through turbulent mixing, while insufficient flow can result in localized oxygen depletion, threatening shrimp health. On the other hand, excessively high flow may lead to DO supersaturation, which can be equally harmful to aquatic life [5]. Therefore, it is essential to evaluate the relationship between aerator parameters (e.g., blade speed, configuration, immersion depth) and pond water flow characteristics, in order to establish best practices for optimizing DO delivery and energy efficiency [6].

Numerous studies have evaluated the performance of mechanical aerators in aquaculture systems, with a focus on their ability to enhance dissolved oxygen (DO) levels through improved water flow dynamics. Peterson and Walker *et al.,* (2002) [7] assessed a real experimental of Taiwanese paddlewheel aerators on a pond and found that increasing rotational speed significantly enhanced oxygen transfer, with standard aeration efficiency

(SAE) ranging from 0.31 to 1.33 kg O_2/kWh and standard oxygen transfer rate (SOTR) rising from 0.31 to 1.34 kg O_2/h as speed increased from 6.5 to 11 rad/s. Roy *et al.,* (2015) [8] further demonstrated that optimal aerator efficiency was achieved at 17rad/s (SAE = 1.019 kg O_2/kWh), while the lowest aeration cost occurred at 8rad/s in smaller ponds (<700 m³), highlighting the importance of matching speed and flow conditions to pond scale.

Moreover, a study develop a new compact paddlewheel hole aerator design reaching SAE values up to 2.54 kg O_2/kWh, while achieved even higher efficiency (SAE of 2.95 kg O_2/kWh) by using CFD-optimized curved blade configurations design that enhanced flow-induced turbulence and oxygen diffusion [9]. These findings underscore how specific design elements such as blade shape, rotor speed, and immersion depth directly influence hydrodynamic behavior and, consequently, DO transfer performance.

Recent innovations have further explored ways to improve flow dynamics while reducing energy demands. Amovable blade paddlewheel aerator that reduces drag and torque by 23–36% depending on immersion depth, lowering required input power to just 0.34 kW which significantly below conventional systems (2.25–7.5 kW) [10] CFD simulations of these systems confirmed enhanced flow uniformity and reduced energy loss. In a broader review, Tanveer *et al.,* (2018) [11] concluded that paddlewheel aerators continue to outperform alternatives like spiral aerators in larger ponds due to their superior SOTR and SAE. Additional studies also show that material selection and blade holes configuration such as using steel over PVC or adopting zigzag and flat designs can significantly improve water movement and oxygen transfer across different pond depths.

Taken together, these studies establish a strong link between aerator designs parameters and the resulting flow conditions within aquaculture ponds, which are critical for effective DO management. This study aims to investigate how key designs and configurations parameters of mechanical aerators will influence water flow dynamics in shrimp ponds, with a focus on identifying best conditions for effective and sustainable DO management.

2.0 METHODOLOGY

2.1 Governing Equation

In this study, a Computational Fluid Dynamics (CFD) approach was employed using FLOW-3D software to simulate the hydrodynamic behavior under investigation. FLOW-3D solves the three-dimensional Navier–Stokes equations for incompressible, viscous flow, incorporating appropriate turbulence and free surface models depending on the physics involved.
The fundamental governing equations used in the simulations are as follows:

Continuity Equation (Mass Conservation): For incompressible flow:

$$\partial u/\partial x + \partial v/\partial y + \partial w/\partial z = 0 \quad \text{(Eqn. 3)}$$

2. Momentum Equations (Navier-Stokes Equations):
In the x-direction:

$$\partial u/\partial t + u(\partial u/\partial x) + v(\partial u/\partial y) + w(\partial u/\partial z) = -1/p\,(\partial p/\partial x) + v(\partial^2 u/\partial x^2 + \partial^2 u/\partial y^2 + \partial^2 u/\partial z^2) + F_x \quad \text{(Eqn. 4)}$$

Where:

- u, v, w: velocity components
- p: pressure
- ρ: fluid density
- $v = \mu/\rho$: kinematic viscosity
- Fx, Fy, Fz: body forces

Free Surface Tracking (Volume of Fluid - VOF method):

$$\partial F/\partial T + \nabla \cdot (F\vec{V}) = 0 \quad \text{(Eqn. 5)}$$

Where:

- F is the fluid volume fraction (0 for empty, 1 for full of fluid)

2.2 CFD Configuration and Parameters

In this study, a numerical CFD using FLOW 3Dsoftware was used to achieve the aims. The approach has been employed in many researching aquaculture systems, proving to be an effective tool for optimizing the performance of mechanical aerators. Some of the article related can be summarized in Table 1.

Table 1 Summarize of review for mechanical aerator

No	Title	Reference
1	CFD Study to Determine the Optimal Configuration of Aerators in a Full-Scale Waste Stabilization Pond	[12]
2	CFD Modelling Pond Dynamic Processes	[13]
3	Feasibility of a Wind-Powered Aeration System for Small-Scale Aquaculture in Developing Countries	[14]
4	Towards a Robust CFD Model for Aeration Tanks for Sewage Treatment	[15]
5	Study on Two Operating Conditions of a Full- Scale Oxidation Ditch Using CFD Model	[16]

In this technique, fluid flow is replicated based on fundamental flow equations like the Navier-Stokes and continuity equation, which are broken down into discrete elements and solved for every computational unit. Employing CFD software parallels the process of arranging an experiment in numerous aspects [17]. If they are not configured accurately to mirror real-world conditions, the outcomes will not accurately represent reality including in aquaculture industries.

In the initial pre-processing phase, an actual paddlewheel parameter, based on reference [18], was used as the basis for modelling in CFD, as represented in Figure 2. Then, a comprehensively analyse of influence of aerator designs into flow characteristics were investigated with three distinct paddle configurations models: a paddle with 12 holes (A) as the basis, paddle with 16 holes (B) and paddle without hole (C), as illustrated in Figures 3 to 5, respectively. These three configurations were selected to evaluate the impact of varying the number and presence of perforations on the paddle's performance, specifically focusing on the effects on flow rate, dissolved oxygen levels, and energy consumption. Although the other parameters were kept constant across all configurations to ensure a controlled comparison, the variations in hole number allowed us to isolate and identify the specific influence of perforations on the overall system performance. This approach helps provide a deeper understanding of how aerator modifications are affected into its efficiency.

The paddles are designed with shafts and connected at the ends with blades. Some parameters were omitted under the assumption that negligible components have minimal impact on fluid flow dynamics. This simplification serves to reduce computational errors associated with discretization during the CFD pre-processing stage.

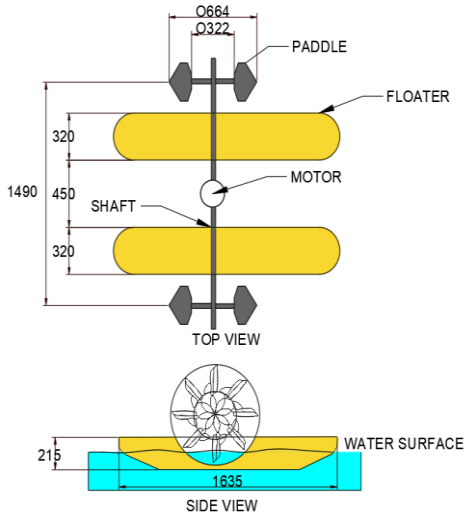

Figure 2 Design of paddlewheel aerator [18]

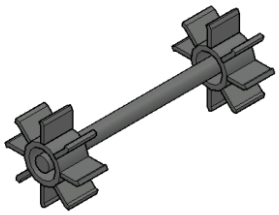

Figure 3 Design of paddlewheel without holes blade

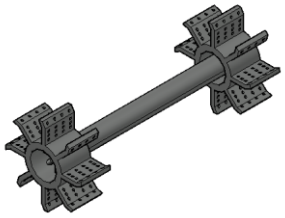

Figure 4 Design of paddlewheel with 16 holes 2.6 cm diameter blade

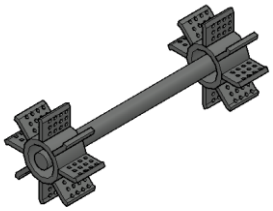

Figure 5 Design of paddlewheel with 12 holes 2.6 cm diameter blade

The subsequent stage involves exporting the models into simulation software. This process entails setting up simulations encompassing physics, fluids, boundaries, viscosity and turbulent condition, mesh, and selecting the most appropriate solver for the cases. The simulation boundary is defined with dimensions of 5m length in x direction, 3m width in y direction and 0.85m depth in z direction. consistence with the basis domain in reference [18] to accommodate the paddle wheel and analyse the flow surrounding the blades. The boundary setups are set for wall at the bed and symmetries in all other directions to avoid the water splashing, as shown in Figure 6.

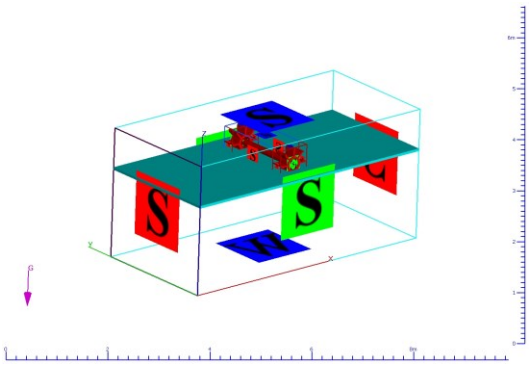

Figure 6 Boundary condition for present model

An RNG turbulence closure have been chosen as turbulence model, since its offers improved accuracy for capturing swirling, recirculating, and rapidly strained flows compared to the others. A time step finish time has been made up to be 0.01 and 30s respectively, due to limited computer storage. Simulations were carried out by using several machines built with Processor Type Intel(R) Core (TM) i7 CPU, 2.67GHz with the RAM capacity is 16Gb.

A mesh convergence study is conducted to ascertain the optimal cell size for the study. Figure 7 to Figure 9 present a mesh convergence study to determine the optimal mesh size for a simulation. Four mesh blocks were tested with varying cell sizes from fine to coarse across five cases (B1–B5). Each case resulted in different total mesh counts, ranging from 3,028,700 to 157,800 cells. Key evaluation criteria included average velocity results, simulation finish time, and storage requirements.

Case B3, with a total mesh of 1,594,000 cells, was selected as the most suitable. It offers a balance between computational efficiency and result accuracy. It's also shows that, the average velocity stabilizes at this mesh size, while finer meshes in B4 and B5 increase simulation time and storage without significant improvement in accuracy. Coarser meshes (B1 and B2) show less reliable velocity values. Thus, B3 ensures a reliable result with manageable resource usage, making it ideal for continued analysis in the study.

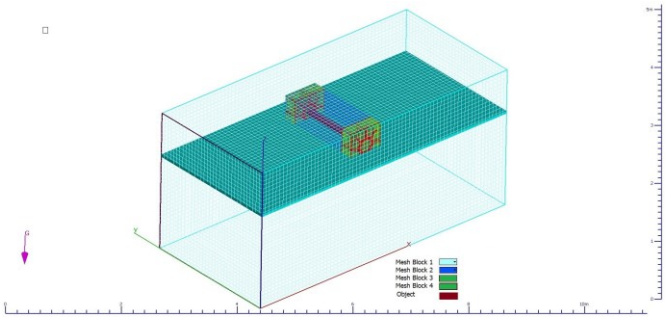

Figure 7 3D view of the computational domain and mesh configuration used in the present model

Cases	Mesh Block 1 (course)	Mesh Block 2 (fine 1)	Mesh Block 3 (fine 2)	Mesh Block 4 (fine 2)	Total Number of Mesh	Finish time (days)	Storage (Gb)	Average Velocity Results (m/s)	Mesh Quality
B1	0.028	0.014	0.007	0.007	3028700	8	23	0.172	Good
B2	0.032	0.016	0.008	0.008	2355500	5	18	0.169	Good
B3	0.036	0.018	0.009	0.009	1594000	3	9	0.183	Good
B4	0.04	0.02	0.01	0.01	955300	2	4	0.151	Good
B5	0.08	0.04	0.02	0.02	157800	1	1	0.128	Bad

Figure 8 Mesh quality of present model

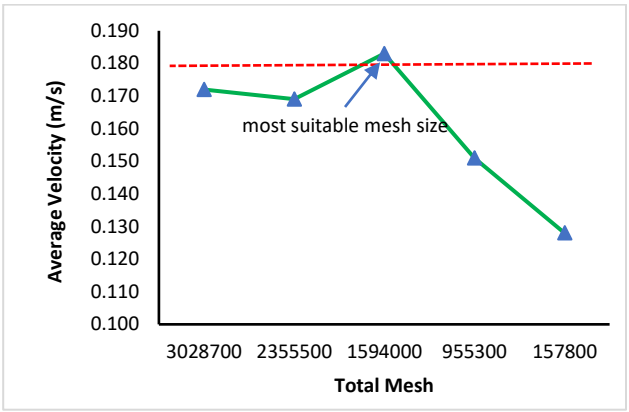

Figure 9 Mesh independence study of present model

The water depth is set at 0.83 m, considering that the paddlewheel blades will be partially submerged as stated by basis design in reference [8]. General Moving Object functionality is activated in the software, with a rotation speed of 12 rad/s for the initial cases (Table 2), followed by various speeds as specified in Table 3. A measurement probe is positioned 1 meter in front of the paddle wheel to assess the water velocity. This measurement is crucial for evaluating the flow rate characteristics of the paddle wheel. The relationship between velocity and flow rate is given by Equation (6):

$$Q=A\cdot V \qquad \text{(Eqn. 6)}$$

where Q represents the flow rate, A is the cross-sectional area of the flow, and V is the measured velocity. The velocity measured by the probe will thus provide insight into the flow rate characteristics, as flow rate is directly proportional to velocity for a constant cross-sectional area.

Table 2 Paddle Wheel types and parameters used in the simulation

Parameters	A	B	C
Diameter	0.67m	0.67m	0.67m
Length	1.5m	1.5m	1.5m
Number of Paddle	8	8	8
Speed	12rad/s	12rad/s	12rad/s
Holes in Paddle	12	16	Non
Holes diameters	0.026	0.026	Non

The test cases of paddle wheel with type A were chosen for further analysis for variation of speeds, as it may operate at different speed capacity.

Table 3 Test cases for variation of paddle wheel speeds

Parameters	Paddle Type A
Diameter	0.67m
Length	1.5m
Number of Paddle	8
Speed	8-16 rad/s
Holes in Paddle	12

To validate the simulation results, reference is made to the experimental study by [18], which investigated water circulation induced by mechanical aerators in a rectangular shrimp aquaculture pond. The study tested a commercial paddle-wheel aerator (TA-55H) with two drums, each equipped with multiple paddles, rotating at approximately 11rad/s. The study reported average velocities exceeding 0.2m/s near the aerator. These measured flow structures and magnitudes provide a reliable benchmark to compare and validate the simulated velocity fields and circulation patterns in this study.

Furthermore, two different wheel paddle configurations (inline and parallel) were investigated to determine the overall effects of paddle wheel contributions on velocity and flow distribution in the pond. Four Paddle A units, each operating at a speed of 12 rad/s, were used in the simulation. The pond was set up with dimensions of 10m by 10m. This dimension choice was due to limited computer capability for running simulations at a full pond scale. Although it does not fully represent the actual pond parameters, it serves as a useful indicator for further studies.

3.0 RESULTS AND DISCUSSION

3.1 Validation

The experimental velocity data from Itano *et al*. (2019) [18] were presented in component form, U_x and U_y. In order to compare the experimental results with the simulation output (velocity magnitude), we calculated the magnitude using Equation (6).

$$V = \sqrt{U_x^2 + U_y^2} \qquad \text{(Eqn. 6)}$$

This conversion allows the experimental and simulated velocity trends to be directly compared in a consistent form. The plotted simulation time was limited to 30 seconds because, as observed in both simulation and experimental results, the flow behavior stabilizes after this period. This timeframe is sufficient to capture the representative hydrodynamic pattern and reduces computational burden. Longer simulations would require high-performance computing resources, which were not available for this study. The setup and simulation decisions are disclosed here to support reproducibility

The comparison between the simulation and experimental data from Itano *et al.* (2019) [18] in Figure 10 shows that both trends are consistent in terms of velocity magnitude and pattern over time. The simulation predicts a gradual increase in velocity, stabilizing around 0.2 m/s, while the experimental data quickly reaches a steady value around 0.25 m/s after an initial spike. To estimate error, the mean absolute error (MAE) over 30 seconds is approximately 0.04–0.06 m/s. The simulation slightly underpredicts peak values but captures the general flow behavior. This close agreement supports the reliability of the simulation in replicating the hydrodynamic performance of the paddle-wheel aerator.

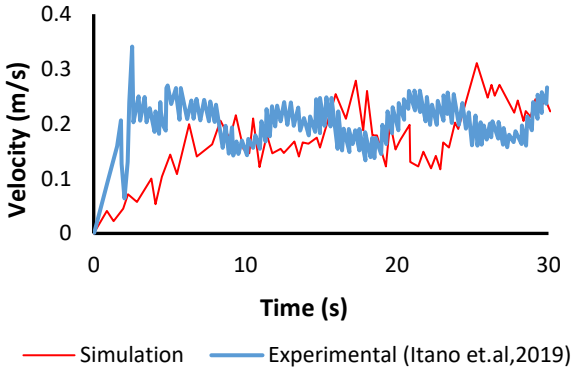

Figure 10 Comparison between the simulation and experimental data from Itano *et al.* (2019) [18]

3.2 Effect of Paddle Hole

In this case, the impact of different paddle wheel designs on fluid velocity, specifically on blades with and without holes was evaluated. Figure 11 shows the time evolution of fluid velocity for each blade design. Initially, the blades without holes exhibit faster fluid velocities due to higher resistance caused by the larger surface area. Conversely, blades with holes allow water to pass through, reducing resistance and enabling lower initial velocities. This aligns with fluid dynamics principles, where reduced surface area and friction facilitate lower on water velocities or flow rates.

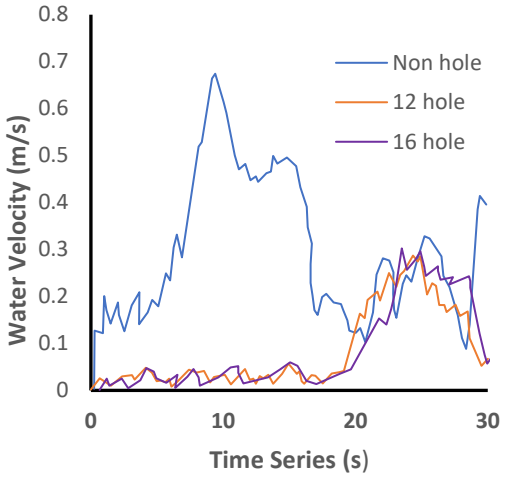

Figure 11 Comparison time series simulation of fluid velocity magnitude of different blades design holes

Furthermore, Figure 12 shows an average of water velocity speed contribute by each blade's designs. Its present blade without holes achieves higher velocity compare to those with holes up to 73.3%. It leading to increased turbulent diffusion of atmospheric oxygen into the water. However, a proper water flow is crucial for maintaining dissolved oxygen levels, essential for the well-being of shrimp populations. And excessively high velocities also could lead to an overabundance of aerated dissolved oxygen, while sluggish flow can decrease oxygen levels, threatening shrimp health.

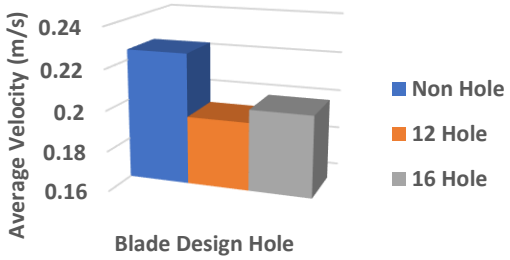

Figure 12 Average Fluid velocity magnitude at stable condition

Figures 13 to 15 provide detailed CFD results that support the study's findings. The data show that paddles with 16 holes generate significantly more water splashing compared to those with 12 holes or no holes. This could fulfil the condition of oxidation process, which indicate that the enhancing the exposing more water to atmospheric oxygen might facilitating better oxygen exchange [19]. It is crucial for maintaining optimal dissolved oxygen levels for shrimp health and growth [20]. Moreover, paddles with holes exhibit a more uniform distribution of fluid velocities/flow rate, essential for efficient water mixing and even oxygen dispersion.

Furthermore, paddle with 16 holes has given low turbulence illustration compare to others designs. It could be harmful to the aquatic environment. The balance achieved by using paddles with 16 holes is particularly noteworthy, as it ensures adequate oxygenation while controlling turbulent diffusion, promoting a healthy habitat for shrimp and minimizing sediment resuspension risks [21].

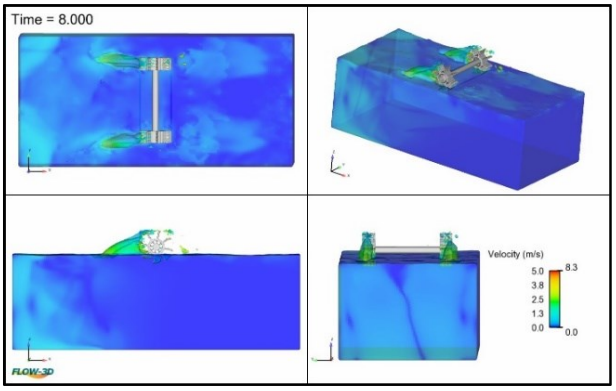

Figure 13 Velocity /flow distribution using paddle with 16 holes

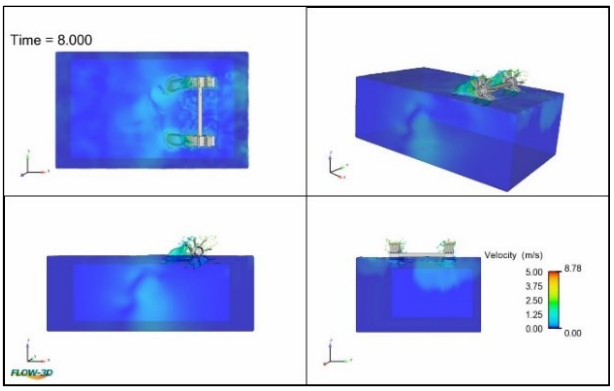

Figure 14 Velocity /flow distribution using paddle with 12 holes

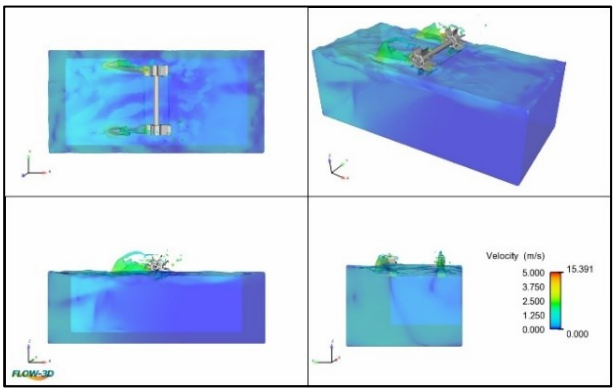

Figure 15 Velocity/flow distribution using paddle without holes

3.3 Effect of Paddle Speed

This study provides a comprehensive analysis of the impact of paddle speed on water velocities or flow rates. Figure 16 illustrates the time series simulation of water velocities at different paddle speeds (8 rad/s to 16 rad/s). All values represented in the figure exhibit fluctuations over time, which is expected due to the complex interaction between the rotating paddle and water. The rotation of the paddlewheel creates periodic pulses of energy, resulting in oscillations in water velocity as each paddle enters and exits the water surface. Higher paddle speeds, such as 16 rad/s, demonstrate more pronounced fluctuations, reflecting the increased frequency and intensity of these pulses, which in turn lead to greater turbulence. This heightened turbulence enhances mixing and oxygenation but can also significantly increase energy consumption and create conditions that may stress or harm aquatic organisms if not properly managed [22].

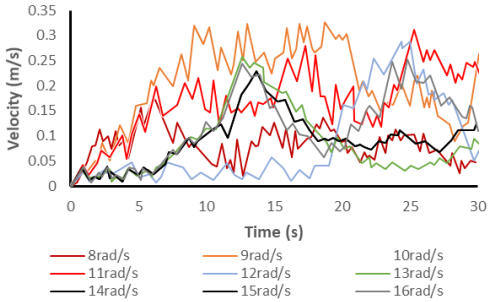

Figure 16 Comparison Effect of paddle speed to the water velocities or flow rate in time series simulation

Furthermore, in Figure 17 shows a non-linear relationship of average water velocities or flow rate for different paddle speed.

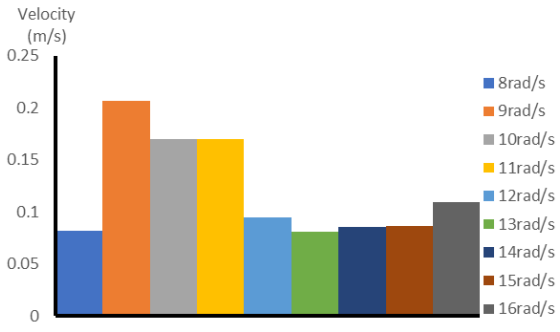

Figure 17 Comparison of an average water velocities or flow rate at different paddle speed

The velocity started with lower at 8 rad/s the rises significantly between 9rad/s to 11 rad/s, then plateaus from 12rad/s to 15rad/s before increasing further at 16 rad/s. The plateau between 9 rad/s and 11 rad/s may indicate a region of optimal energy transfer efficiency, where increased energy input does not proportionally increase water velocity due to turbulence and energy losses. The sharp increase at 16 rad/s suggests a threshold overcoming these losses, leading to higher velocities but also greater turbulence. These findings highlight the balance needed between paddle speed, efficient mixing, and energy consumption for optimal aquatic environment management.

3.4 Effect of Paddle Configuration

The effects of different paddle configurations on pond water velocity or flow rate distribution analysed to assess their impact on hydrodynamic performance. Figure 14 shows that the parallel paddle configuration creates multiple high-velocity zones with maximum velocity 13.4m/s, indicating effective water movement and extensive mixing.

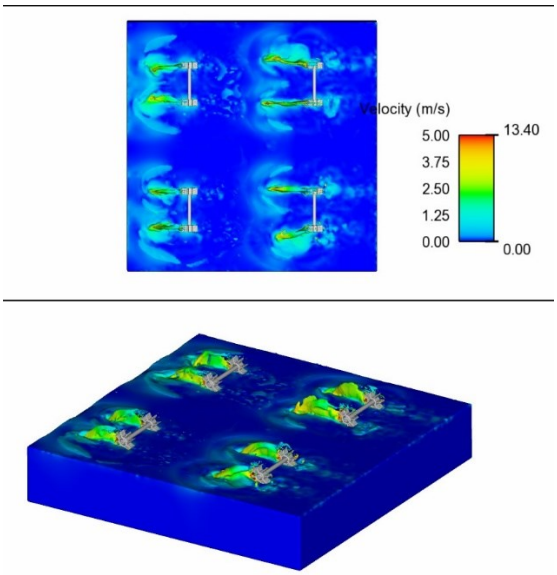

Figure 14 Effect of parallel paddle configuration on pond water velocity or flow rate distribution

This setup ensures each paddle contributes to a uniform distribution of kinetic energy, enhancing overall water circulation within the pond. Such uniformity is crucial for large aquaculture systems, as it ensures consistent oxygen distribution, maintaining a healthy environment for aquatic life [23]. The extensive mixing promoted by the parallel configuration helps reduce the likelihood of low-oxygen areas, which is beneficial for sustaining shrimp populations [21]. The parallel configuration is particularly effective in preventing stratification, which can lead to stagnant zones and poor water quality. Additionally, the parallel paddles create moderate turbulence, which helps distribute oxygen more evenly without causing excessive stress on the aquatic organisms.

In contrast, Figure 15 demonstrates that the inline paddle configuration results in a concentrated high-velocity zone along the paddles' path with water velocity up to 34.53m/s. This setup generates a streamlined flow pattern, with high velocities near the paddles that decrease further away. While this configuration can effectively facilitate localized mixing and aeration, it may not achieve the same level of uniform water movement throughout the pond as the parallel configuration [24]. The inline configuration may be more efficient in targeted applications where specific areas require higher oxygen levels and mixing intensity. However, it might not prevent the formation of low-oxygen zones as effectively as the parallel configuration [25]. The inline setup generates higher localized turbulence, which can enhance oxygenation in specific regions but might also lead to increased energy consumption and stress on aquatic organisms if not properly managed [26]. The choice between these configurations depends on the specific needs of the aquaculture system: parallel paddles for widespread mixing and oxygenation, and inline paddles for targeted aeration and energy efficiency [27].

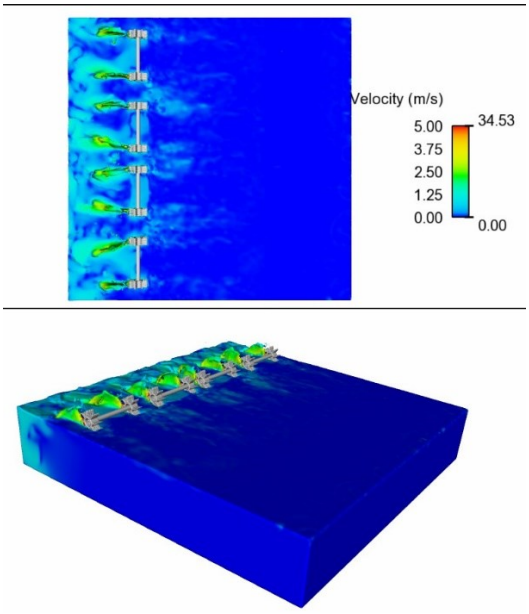

Figure 15 Effect of inline paddle configuration on pond water velocity or flow rate distribution

4.0 CONCLUSION

The investigation into the parameters of mechanical aerators and their effects on pond water flow rates using CFD has provided significant insights. The study revealed that aerator speed is directly proportional to the water flow rate, with a paddle optimal speed range of 9 rad/s to 11 rad/s for balanced performance. Paddlewheel designs also play a crucial role, with aerators without holes achieving up to 73.3% higher flow rates compared to those with holes, which leading to increased turbulent diffusion of atmospheric oxygen into the water. However, uncontrolled water velocity of flow rates could lead to the death of shrimp.

These findings underscore the importance of optimizing both the design and operational parameters of mechanical aerators to enhance water quality in aquaculture systems. The results advocate for further exploration and refinement of these parameters to achieve optimal practices for mechanical aerators, ensuring efficient energy use and promoting a healthy aquatic environment. This research provides a foundation for future studies aimed at improving mechanical aeration practices in shrimp pond management.

For future work, we recommend extending the simulation time and employing higher computational capabilities to capture full periodic flow patterns and unsteady effects over a longer time horizon. This would help enhance the understanding of transient phenomena and improve the fidelity of CFD models for aquaculture aerators

Acknowledgement

The authors gratefully acknowledge the CAD training support provided under the KTAGS Grant (UMT/PPJIM/2-2/25/15/JLD 5 – Vot No. 58926) and the financial assistance from the Research Management Office, UMT. The authors also extend their sincere appreciation to all staff members of the Department of Marine Technology and Naval Architecture for their invaluable support and cooperation throughout the course of this study.

Conflicts of Interest

The authors declare that there is no conflict of interest regarding the publication of this paper.

References

[1] Bhuyar, L., S. Thakre, and N. Ingole. 2010. Design Characteristics of Curved Blade Aerator w.r.t. Aeration Efficiency and Overall Oxygen Transfer Coefficient and Comparison with CFD Modeling. *International Journal of Engineering Science and Technology*. 1(1): 1–15. https://doi.org/10.4314/ijest.v1i1.58055.

[2] Moore, J. M., and C. E. Boyd. 1992. Design of Small Paddle Wheel Aerators. *Aquacultural Engineering*. 11(1): 55–69. https://doi.org/10.1016/0144-8609(92)90021-O.

[3] Ma, L., C. Jiang, D. Li, H. Zhang, and Z. Li. 2021. Terrain Pre-Process the Lower Reaches Yellow River and Delta Estuary Coast of Two Dimensional Numerical Model. *Journal of Physics: Conference Series*. 1885(5): 052041. https://doi.org/10.1088/1742-6596/1885/5/052041.

[4] Baylar, A., T. Bagatur, and M. E. Emiroglu. 2007. Prediction of Oxygen Content of Nappe, Transition, and Skimming Flow Regimes in Stepped-Channel Chutes. *Journal of Environmental Engineering and Science*. 6(2): 201–208. https://doi.org/10.1139/S06-048.

[5] Gu, Y., Y. Li, F. Yuan, and Q. Yang. 2023. Optimization and Control Strategies of Aeration in WWTPs: A Review. *Journal of Cleaner Production*. 418: 138008. https://doi.org/10.1016/j.jclepro.2023.138008.

[6] Mugo-Bundi, J., J. O. Manyala, M. Muchiri, and G. Matolla. 2024. Effects of Stocking Density and Water Flow Rate on Performance, Water Quality and Economic Benefits of African Catfish Larvae (*Clarias gariepinus* Burchell, 1822) in the Aquaponic System Integrated with Azolla Fern. *Aquaculture*. 579: 740170. https://doi.org/10.1016/j.aquaculture.2023.740170.

[7] Peterson, E. L., and M. B. Walker. 2002. Effect of Speed on Taiwanese Paddlewheel Aeration. *Aquacultural Engineering*. 26(2): 129–147. https://doi.org/10.1016/S0144-8609(02)00009-2.

[8] Roy, S. M., S. Moulick, C. K. Mukherjee, and B. C. Mal. 2015. Effect of Rotational Speeds of Paddle Wheel Aerator on Aeration Cost. *American Research Thoughts*. 2(1): 3069–3087.

[9] Bahri, S., R. P. Setiawan, W. Hermawan, and M. Zairin Junior. 2015. Simulation on Blade Geometry and Operational Condition toward Torque Requirement and Drag Force in Paddle Wheel Aerator. *International Journal of Scientific and Engineering Research*. 6(2): 812–816.

[10] Arini, N. R., M. U. Al Ala, W. R. Kusuma, M. A. Mubarok, and M. B. Sigalo. 2023. Numerical Study on the Effect of Wheel Aerator Paddle Profiles to Fluid Flow Characteristics and Aeration Performance Prediction. In *International Electronics Symposium 2023*. 1–6. https://doi.org/10.1109/IES59143.2023.10242477.

[11] Tanveer, M., S. M. Roy, M. Vikneswaran, P. Renganathan, and S. Balasubramanian. 2018. Surface Aeration Systems for Application in Aquaculture: A Review. *International Journal of Fisheries and Aquatic Studies*. 6(5): 342–347.

[12] Alvarado, A., M. Vesvikar, J. F. Cisneros, T. Maere, P. Goethals, and I. Nopens. 2013. CFD Study to Determine the Optimal Configuration of Aerators in a Full-Scale Waste Stabilization Pond. *Water Research*. 47(13): 4528–4537. https://doi.org/10.1016/j.watres.2013.05.016.

[13] Peterson, E. L., J. A. Harris, and L. C. Wadhwa. 2000. CFD Modelling Pond Dynamic Processes. *Aquacultural Engineering*. 23 (1–3): 61–93. https://doi.org/10.1016/S0144-8609(00)00050-9.

[14] Mahmudov, K., A. Mahmoud, S. Sur, F. C. Cruz, and A. M. Bilton. 2019. Feasibility of a Wind-Powered Aeration System for Small-Scale Aquaculture in Developing Countries. *Energy for Sustainable Development*. 51: 40–49. https://doi.org/10.1016/j.esd.2019.05.003.

[15] Karpinska Portela, A. M., and J. Bridgeman. 2017. Towards a Robust CFD Model for Aeration Tanks for Sewage Treatment—A Lab-Scale Study. *Engineering Applications of Computational Fluid Mechanics*. 11(1): 371–395. https://doi.org/10.1080/19942060.2017.1307282.

[16] Yang, Y., *et al*. 2011. Study on Two Operating Conditions of a Full-Scale Oxidation Ditch for Optimization of Energy Consumption and Effluent Quality by Using CFD Model. *Water Research*. 45: 3439–3451. https://doi.org/10.1016/j.watres.2011.04.007.

[17] Basso, A., F. A. Hamad, and P. Ganesan. 2019. Initial Results from the Experimental and Computational Study of Microbubble Generation. In *4th World Congress on Momentum, Heat and Mass Transfer*. 1–9. https://doi.org/10.11159/icmfht19.101.

[18] Itano, T., *et al*. 2019. Water Circulation Induced by Mechanical Aerators in a Rectangular Vessel for Shrimp Aquaculture. *Aquacultural Engineering*. 85: 106–113. https://doi.org/10.1016/j.aquaeng.2019.03.006.

[19] Li, D., M. Zou, and L. Jiang. 2022. Dissolved Oxygen Control Strategies for Water Treatment: A Review. *Water Science and Technology*. 86(6): 1444–1466. https://doi.org/10.2166/wst.2022.281.

[20] Xue, B., Y. Zhao, C. Bi, Y. Cheng, X. Ren, and Y. Liu. 2022. Investigation of Flow Field and Pollutant Particle Distribution in the Aquaculture Tank for Fish Farming Based on Computational Fluid Dynamics. *Computers and Electronics in Agriculture*. 200: 107243. https://doi.org/10.1016/j.compag.2022.107243.

[21] Kurniawan, S. B., *et al*. 2021. Aquaculture in Malaysia: Water-Related Environmental Challenges and Opportunities for Cleaner Production. *Environmental Technology & Innovation*. 24: 101913. https://doi.org/10.1016/j.eti.2021.101913.

[22] Verma, D. K., N. K. Maurya, and P. Kumar. 2022. Important Water Quality Parameters in Aquaculture: An Overview. *Agriculture and Environment*. 3: 24–29.

[23] Chaparala, V., R. K. S. Gadepalli, and P. P. Parvathaneni. 2023. A Molecular Dynamics Approach for a Parametric Study of Colloidal Suspension Aggregation Kinetics. *International Journal on Interactive Design and Manufacturing*. https://doi.org/10.1007/s12008-023-01309-5.

[24] Martin, T., A. Kamath, G. Wang, and H. Bihs. 2022. Modelling Open Ocean Aquaculture Structures Using CFD and a Simulation-Based Screen Force Model. *Journal of Marine Science and Engineering*. 10(3): 332. https://doi.org/10.3390/jmse10030332.

[25] Roy, S. M., S. Moulick, and B. C. Mal. 2017. Design Characteristics of Spiral Aerator. *Journal of the World Aquaculture Society*. 48(6): 898–908. https://doi.org/10.1111/jwas.12410.

[26] Ranga Rao, A., and A. R. Gokare. 2022. *Sustainable Global Resources of Seaweeds. Volume 1: Bioresources, Cultivation, Trade and Multifarious Applications*. Cham: Springer. https://doi.org/10.1007/978-3-030-91955-9.

[27] Anuar, F. F., B. A. M. Zain, and S. Abdullah. 2020. The Improvement of Flexible Aerator Parameter to Increase Dissolved Oxygen Level in Freshwater. *International Journal of Integrated Engineering*. 12(3): 197–206. https://doi.org/10.30880/ijie.2020.12.03.023.